EDCSMOKE: A NEW COMBUSTION SOLVER BASED ON OPENFOAM

M. R. Malik*, Z. Li*, A. Cuoci** and A. Parente*

Zhiyi.Li@ulb.ac.be

*Université Libre de Bruxelles, Ecole Polytechnique de Bruxelles, Aero-Thermo-Mechanics Laboratory, Belgium

**Department of Chemistry, Materials, and Chemical Engineering ”G.Natta”, Politecnico di Milano, Italy

Abstract

A new OpenFOAM solver for combustion problems requiring detailed kinetic mechanisms is presented. The Eddy Dissipation Concept (EDC) is used as the turbulence-chemistry interaction model. The solver, called ”edcSimpleSMOKE” for the steady-state and ”edcPimpleSMOKE” for the unsteady form, was developed recently for a robust handling of large and detailed chemical mechanisms. The solver was validated using high-fidelity experimental data from several flames: the piloted methane-air Sandia flame D, the Sandia/ETH-Zurich $CO/H_2/N_2$ flames A & B, the DLR/TU/Sandia $CH_4/H_2/N_2$ flame (DLR A), the Sandia/ETH H_2/He flame and the Adelaide Jet in Hot Co-flow (JHC) flame. In general, satisfactory agreement is found between the simulations and the experimental results, for both temperature and species concentrations profiles. What's more, a comparison is made between the different formulations of the EDC model.

Introduction

The numerical modelling of turbulent combustion is a very challenging task as it combines the complex phenomena of turbulence and chemical reactions. Studying the effects of turbulence is already a complex task as turbulence is a classical unsolved physical phenomenon. If turbulence is then coupled with chemical reactions, this study becomes even more challenging as the interactions between a macro level phenomenon (turbulence) and a molecular one (chemical reactions) have to be treated simultaneously in the modelling procedure. This study becomes again even more challenging when large detailed kinetic mechanisms are used in order to understand some special features such as pollutant formation.

The purpose of the present work is to implement a new stable solver for OpenFOAM capable of using detailed chemical reaction mechanisms. The turbulence-chemistry interaction is handled with the Eddy Dissipation Concept (EDC) of Magnussen [1] . Based on reactingFoam, the solver was developed both under the steady-state form (”edcSimpleSMOKE”) and the unsteady form (”edcPimpleSMOKE”). Moreover, the solver is coupled with the OpenSMOKE library developed by Cuoci [2] for the integration of detailed chemistry.It is specially developed to manage large, detailed kinetic schemes in CFD simulations of reacting flows. The purpose of this paper is to present the validation of the solver using experimental data from several flames.

Eddy Dissipation Concept for turbulent combustion

The Eddy Dissipation Concept (EDC), developed by Magnussen [1, 3, 4], is an extension of the Eddy Dissipation Model (EDM) [5] to finite rate chemistry, allowing the inclusion of detailed chemical mechanisms in turbulent flows. Based on the energy cascade model, the

EDC model gives an empirical expression for the mean reaction rate based on the assumption that chemical reactions occur in the regions of the flow where the dissipation of turbulence energy takes place. In turbulent flows, molecular mixing and dissipation of turbulence energy into heat are concentrated in isolated regions occupying a fraction of the total volume of the fluid. These regions are called fine structures. These fine structures are believed to be vortex tubes, sheets or slabs with characteristic dimensions of the order of the Kolmogorov length scale [4]. The Kolmogorov length scale, η, defined as:

$$\eta = \left(\frac{\nu^3}{\epsilon}\right)^{1/4},$$

where ν is the kinematic viscosity and ϵ is the dissipation of turbulent kinetic energy k. The fine structures are responsible for the dissipation of turbulence energy into heat as well as for the molecular mixing. The mass fraction of the fine structures, γ_λ, and the mean residence time of the fluid within them, τ^*, are provided by an energy cascade model [6], which describes the energy dissipation process as a function of the characteristic scales:

$$\gamma_\lambda = \left(\frac{3C_{D2}}{4C_{D1}^2}\right)^{\frac{1}{4}} \left(\frac{\nu\epsilon}{k^2}\right)^{\frac{1}{4}} = C_\gamma \left(\frac{\nu\epsilon}{k^2}\right)^{\frac{1}{4}}, \tag{1}$$

and

$$\tau^* = \left(\frac{C_{D2}}{3}\right)^{\frac{1}{2}} \left(\frac{\nu}{\epsilon}\right)^{\frac{1}{2}} = C_\tau \left(\frac{\nu}{\epsilon}\right)^{\frac{1}{2}}, \tag{2}$$

where ν is the kinematic viscosity and ϵ is the dissipation of turbulent kinetic energy, k. C_{D1} and C_{D2} are model constants set equal to 0.135 and 0.5, respectively, leading to fine structure volume and residence time constants equal to $C_\gamma = 2.1377$ and $C_\tau = 0.4083$. Fine structures are assumed to be isobaric, adiabatic perfectly stirred reactors.

The expression for the mean source term in the species conservation equation has different formulations. Initially, in the first publication on the EDC, the mean source term in the conservation equation for the kth species was modeled by Magnussen as follows [3]:

$$\overline{\dot{\omega}}_k = -\frac{\overline{\rho}\gamma_\lambda^3}{\tau^* \left(1 - \gamma_\lambda^3\right)} \left(\widetilde{y}_k - y_k^*\right), \tag{3}$$

where $\overline{\rho}$ denotes the mean density of the mixture, y_k^* is the mass fraction of the kth species in the fine structures and $\widetilde{y}_k$ represents the mean mass fraction of the kth species between the fine structures and the surrounding state (indicated as y_k^0):

$$\widetilde{y}_k = \gamma_\lambda^3 y_k^* + \left(1 - \gamma_\lambda^3\right) y_k^0. \tag{4}$$

This will be called "EDC_old" in the remaining of this paper. In 1996, Magnussen argued that as the fine structures exchange mass with the fine-structure regions, the mass exchange between the fine structures and the surroundings should be modelled as $\frac{\gamma_\lambda^2}{\tau^*}$. The mean source term is then modelled as [7]:

$$\overline{\dot{\omega}}_k = -\frac{\overline{\rho}\gamma_\lambda^2}{\tau^* \left(1 - \gamma_\lambda^3\right)} \left(\widetilde{y}_k - y_k^*\right). \tag{5}$$

This is the formulation of the EDC used in the commercial code Fluent. Therefore, it will be called "EDC_fluent" subsequently. In 2005, Magnussen modified his model again, suggesting than the mean source term should now be modelled as [1]:

$$\overline{\dot{\omega}}_k = -\frac{\overline{\rho}\gamma_\lambda^2}{\tau^* \left(1 - \gamma_\lambda^2\right)} \left(\widetilde{y}_k - y_k^*\right),$$
(6)

and the mean mass fraction of the kth species between the fine structures and the surrounding state becomes:

$$\widetilde{y}_k = \gamma_\lambda^2 y_k^* + \left(1 - \gamma_\lambda^2\right) y_k^0.$$
(7)

This formulation will be named "EDC_new".

In all three EDC formulations presented, the mean mass fraction for each species $(\widetilde{y}_k)$ is calculated by solving the species transport equation whereas the mass fraction of each species inside the fine structures (y_k^*) is computed using the detailed chemistry approach.

The EDC Detailed Chemistry approach
In the detailed (or finite-rate) chemistry approach, the effects of chemical kinetics are taken into account by treating the fine structures as constant-pressure adiabatic and homogeneous reactors. Such a reactor is described by:

$$\frac{dy_k^*}{dt} = \omega_k^* + \frac{1}{\tau^*}(y_k^0 - y_k^*), k = 1, ..., n_s$$
(8)

where ω_k^* is the reaction rate of specie k calculated with a detailed mechanism and y_k^0 is the mass fraction of species k entering the reactor (i.e. the mass fraction of species k in the surrounding state) and n_s is the number of species in the chosen kinetic mechanism. Eq. (8) represents a set of ODEs whose solution gives the mass fraction of species inside the fine structures (y_k^*). If a large and detailed mechanism is used, this set of ODEs can become very stiff and its resolution computationally expensive. Magnussen further assumes that the reactors are in steady-state [7], leading to the following set of equations for the mass fractions:

$$\omega_k^* = \frac{(y_k^0 - y_k^*)}{\tau^*}, k = 1, ..., n_s$$
(9)

This gives a set of non-linear algebraic equations obtained by integrating Eq. (8) until the steady-state solution is reached. The solution of Eq. (9) can be substituted in the mean source term (Eq. (3) or (5) or (6)). In this study, several large kinetic mechanisms will be used in order to demonstrate the robustness of the present solver.

Validation test cases
In order to assess the performance of the solver, several test cases with high fidelity experimental data are needed.

Sandia Flame D
Flame D is a piloted methane-air diffusion flame with an axi-symmetric geometry. The main jet (d=7.2mm) consists of 25% of CH_4 and 75% of air (by volume) at a speed of 49.6 m/s and a Reynolds number of Re=22400. This main jet is surrounded by a pilot jet (18.2mm) which is a mixture of C_2H_2, H_2, air, CO_2 and N_2 at 11.4 m/s and 1880K. All this is surrounded by a light coflow of outside air at 0.9 m/s and 291K. The available experimental data consist of

the mean and root mean square (rms) of temperature and mass fractions of major and minor species. A steady-state and 3D axi-symmetric simulation is carried out due to the symmetry of the system. The mesh is structured and nonuniform with about 4,600 cells. The standard $k - \epsilon$ model is used as turbulence model. Two kinetic schemes are used here: the GRI-3.0 mechanism (53 species, 325 reactions) [8], and the Polimi C1C3HTNOX mechanism (115 species, 2142 reactions) [9]. Radiation is also taken into account through the P1 model.

Sandia/ETH-Zurich CO/H2/N2 Flame

The $CO/H_2/N_2$ flames [10, 11, 12] are two turbulent non-premixed jet flames (flame A and flame B) with different nozzle diameter but equal Reynolds number. The fuel composition for both flames is 40% CO, 30% H_2, 30% N_2 by volume. These flames are unconfined and no pilot is necessary to stabilize them. Flame A has a fuel nozzle diameter of 4.58 mm and a velocity of 76 m/s, whereas flame B has a fuel nozzle diameter of 7.72 mm and a velocity of 45 m/s, which results in both cases to a Reynolds number of 16,700. The temperature of the fuel jet is 292K for both cases. The coflow of air is at 290K and has a velocity of 0.70 m/s. The computational domain is 3D axi-symmetric. The mesh is structured and nonuniform with about 5,000 cells for both flame A and flame B. The kinetic scheme used here is the Polimi COH2NOx [13] involving 32 species and 174 reactions. The standard $k - \epsilon$ epsilon model is used as turbulence model and radiation is also taken into account through the P1 model.

DLR/TU/Sandia CH4/H2/N2 flame

A simple jet flame of 22.1% CH_4, 33.2% H_2 and 44.7% N_2 (by volume) in a low-velocity coflow of air [14] is also used in the validation of the edcSmoke solver. The burner has the fuel jet nozzle diameter of 8 mm and fuel velocity of 42.2 m/s (Re=15,200). The fuel jet tube is surrounded by a contoured nozzle supplying dry air coflow with a velocity of 0.3 m/s. The computational domain is 3D axi-symmetric. The mesh is structured and nonuniform with about 3,500 cells. The standard $k - \epsilon$ model is used as turbulence model. The kinetic scheme used for this case is the GRI-3.0 mechanisms (53 species, 325 reactions) [8]. Radiation is modelled using the P1 model.

Sandia/ETH H2/He flame

The Sandia/ETH H_2/He flames [15, 16, 17] are three nonpremixed jet flames: undiluted H_2, 20% He dilution and 40% He dilution. In this study, only the case with 40% dilution was investigated. The burner consists of a straight tube centered at the exit of a vertical wind tunnel contraction. The fuel jet nozzle has a diameter of 3.75 mm. The fuel exit temperature is 295K with a velocity of 256 m/s. The coflow air velocity is 1.0 m/s with a temperature of 294K. A 3D axi-symmetric computational domain is used. The mesh is structured and nonuniform with about 3,000 cells. The standard $k - \epsilon$ epsilon model is used and turbulence radiation is modelled by the P1 approximation. The kinetic scheme used is the Polimi H2/CO with 32 species and 174 reactions [13].

Adelaide JHC flame

The validation test cases introduced above belong to the category of flame combustion. The Adelaide JHC burner [18] emulates the conditions of flameless combustion, also known as MILD (Moderated or Intense Low oxygen Dilution) combustion. Such a regime is characterized by very strong turbulence-chemistry interactions, thus making finite rate chemistry effects more important. The Adelaide JHC burner has a central jet with the equi-molar mix-

ture of CH_4 and H_2. The hot co-flow is provided with four secondary burners in the annulus region. Nitrogen is introduced in to the annulus region as well, in order to control the oxygen level to 3%. The central jet diameter is 4.25 mm, and $Re = 10,000$. In the simulation work, the transient version of the solver 'edcPimpleSMOKE' was used. $k - \varepsilon$ model was selected for turbulence and radiation was turned off. Three different detailed mechanisms, KEE (17 species, 58 reactions) [19], GRI3.0 and San-Diego (50 species, 247 reactions) [20] were tested with the current solver.

Results

This section presents the results obtained for the different test cases. Firstly, the steady state solver was validated against experimental data of two Sandia flames: the piloted flame D and the Sandia/ETH-Zurich $CO/H_2/N_2$ (syngas) flames A & B. For this purpose, the new formulation of the EDC (EDC_new) was used for the turbulence/chemistry interactions model. Secondly, the formulation used in commercial code Fluent (EDC_fluent) was tested with the JHC flameless combustion burner. The transient solver was used for validation. Once the solver was validated, the three formulations of the EDC were compared to each other on two different flames: the DLR/TU/Sandia $CH_4/H_2/N_2$ flame (DLR A) and the JHC burner flame.

Validation of the solver
The objective of this part of the work is to assess the performance of the new solver. Figure 1 shows the radial temperature profiles at different axial locations (a-e) and the centerline profile (f), for flame D, obtained with two different kinetic mechanisms. In general, relatively good agreement between predictions and experimental data can be observed. Moreover, it can be seen that the predictions from both mechanisms are comparable to each other. At axial locations downstream of $x/d = 45$, both mechanisms give the same results whereas some discrepancies are found upstream this location between the GRI-3.0 and Polimi C1C3HTNOX mechanisms. The solver handles well large kinetic schemes, showing deviations between numerical predictions and experimental data only on the locations close to the burner exit ($x/d = 15$ and $x/d = 30$). The predictions of CO_2 are also shown. Figures 2 shows that CO_2 profile is similar with the mean temperature profile, except at the $x/d = 45$ axial location that there is an over-prediction of CO_2 in the region close to the centerline.

Next, the data from syngas flames (Flame A & B) was used to further validate the solver. Figures 3 and 4 show the temperature profiles for flame A and flame B respectively, at different locations. Here again, some deviations are found close to the burner exit plane, but further downstream the agreement is satisfactory for both flames, especially flame B. The solver captures well temperature peaks, with small over-predictions at some locations, mainly for flame A. For flame B, the predictions at $x/d = 40$ and further downstream are generally good near the axis of the burner as well as far from it. Along the centerline, the solver captures well the global temperature profile, together with the peak (both in intensity and position, Figure 4f). The computed mass fraction profiles of NO for flame A are shown on Figure 5, showing some under-predictions at $x/d = 50$, $x/d = 60$ and centerline.

Furthermore, the solver was tested on the JHC burner, to access its applicability in flameless combustion. The EDC_fluent version combined with modified k-epsilon model was adopted here. In the modified k-epsilon model, the $C_{1\epsilon}$ value is adjusted from the default $C_{1\epsilon} = 1.44$ to $C_{1\epsilon} = 1.60$. In Fig. 6, the simulation results of the mean temperature profiles

are compared with the experimental values. There is a fairly good match for the profiles at axial position of 30 mm and along the centerline. Some over-predictions of the temperature peak can be observed for the axial positions of 60 mm and 120 mm, especially at 120 mm. This is consistent with other literature investigations [21]. The similar trend is observed for the H_2O mass fraction (see Fig. 7).
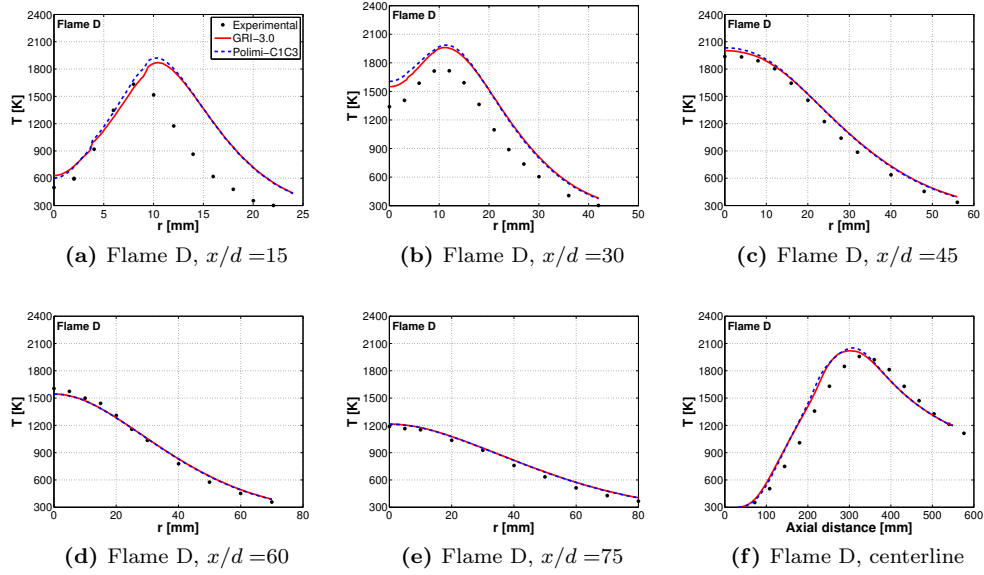

(a) Flame D, $x/d = 15$

(b) Flame D, $x/d = 30$

(c) Flame D, $x/d = 45$

(d) Flame D, $x/d = 60$

(e) Flame D, $x/d = 75$

(f) Flame D, centerline

Figure 1: Comparison of measured and computed temperature profiles at different locations, for flame D

(a) Flame D, $x/d = 15$

(b) Flame D, $x/d = 30$

(c) Flame D, $x/d = 45$

(d) Flame D, $x/d = 60$

(e) Flame D, $x/d = 75$

(f) Flame D, centerline
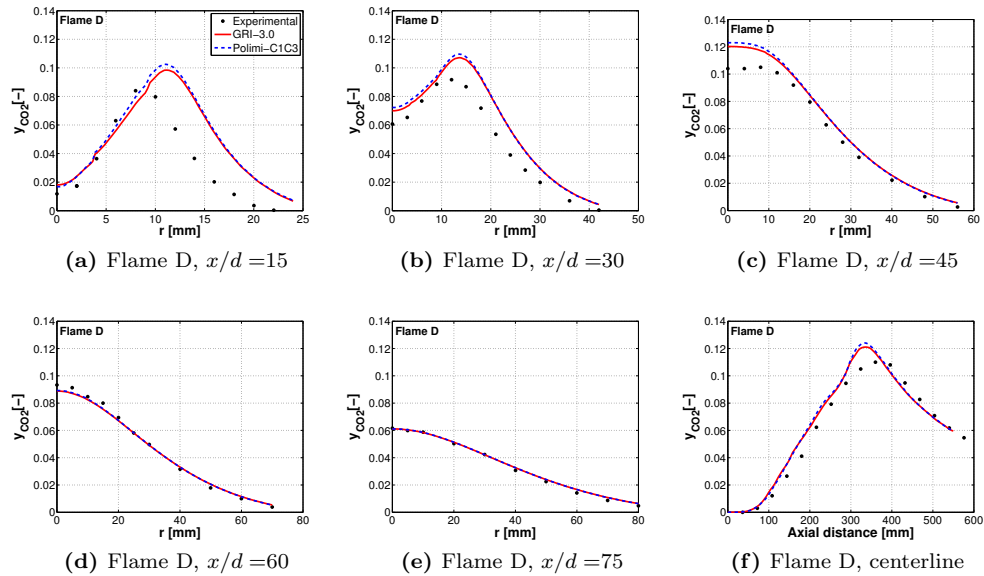
Figure 2: Comparison of measured and computed CO2 mass fraction profiles at different locations, for flame D

(a) Flame A, x/d =20
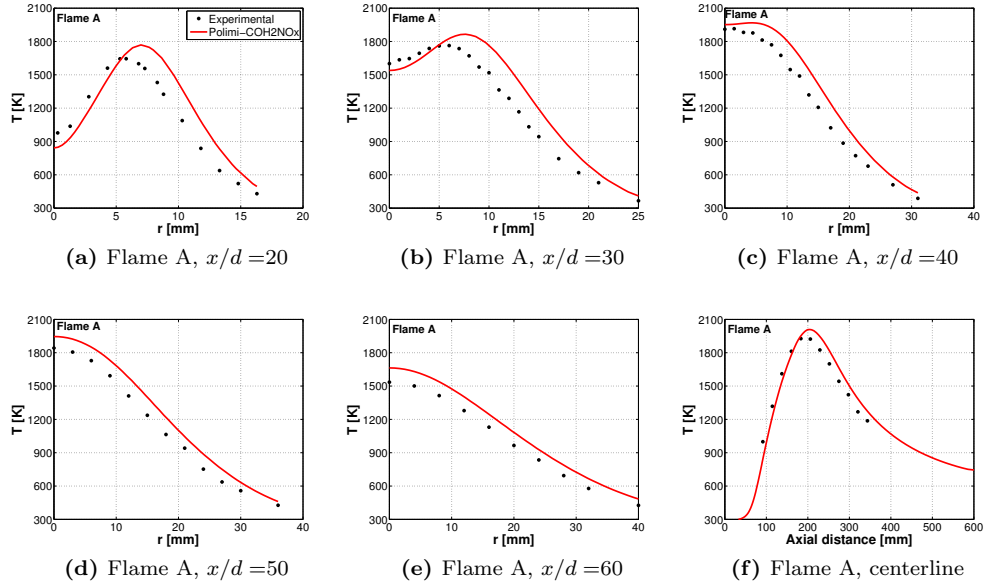
(b) Flame A, x/d =30

(c) Flame A, x/d =40

(d) Flame A, x/d =50

(e) Flame A, x/d =60

(f) Flame A, centerline

Figure 3: Comparison of measured and computed temperature profiles at different locations, for flame A

(a) Flame B, x/d =20

(b) Flame B, x/d =30

(c) Flame B, x/d =40

(d) Flame B, x/d =50

(e) Flame B, x/d =60

(f) Flame B, centerline
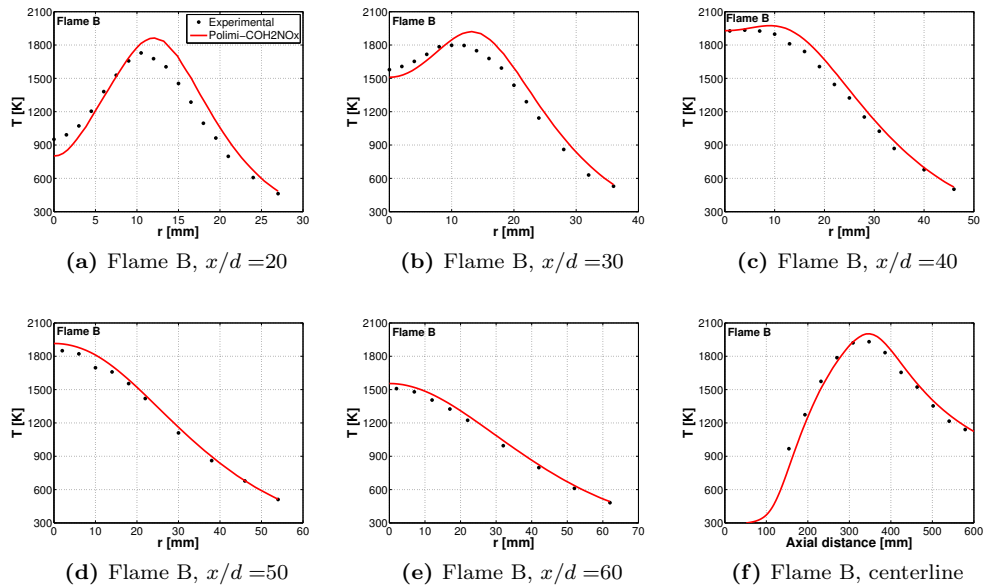
Figure 4: Comparison of measured and computed temperature profiles at different locations, for flame B
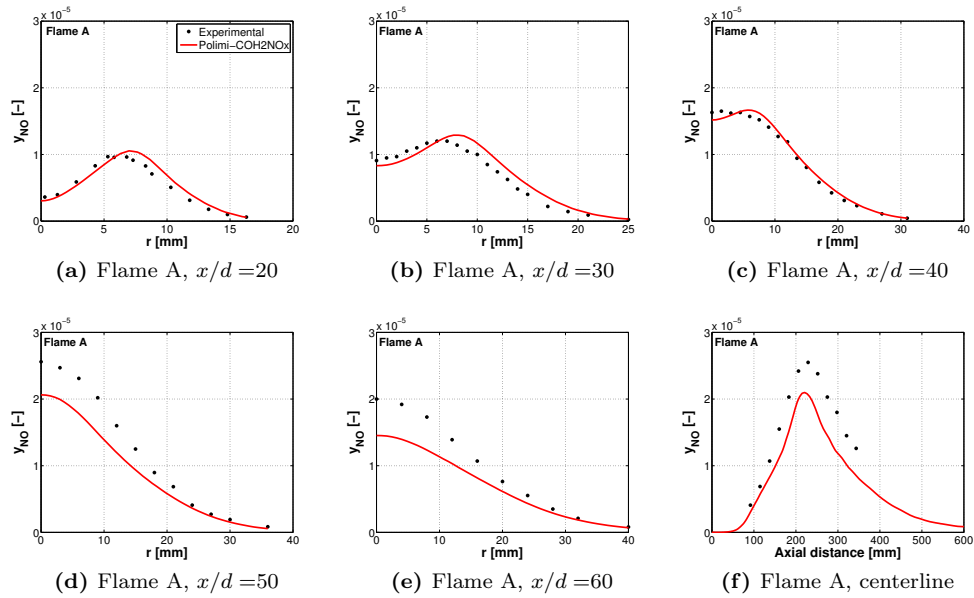
Figure 5: Comparison of measured and computed NO mass fraction profiles at different locations, for flame A
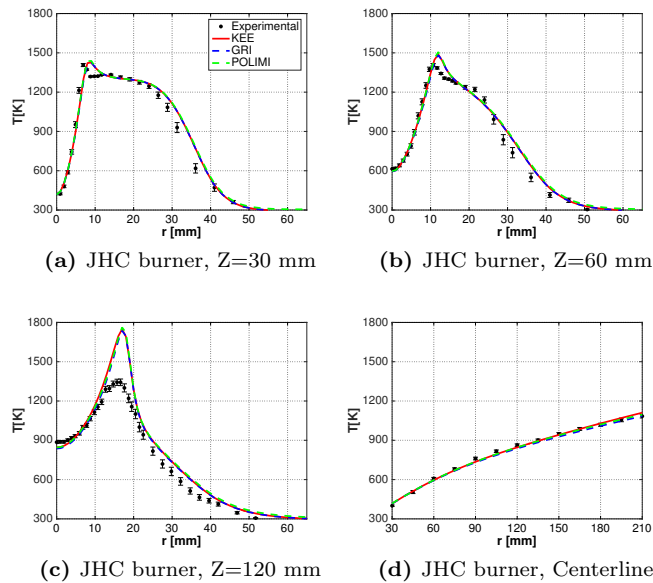

Figure 6: Comparison of measured and computed temperature profiles at different locations, for JHC burner flameless combustion (modified k-epsilon)
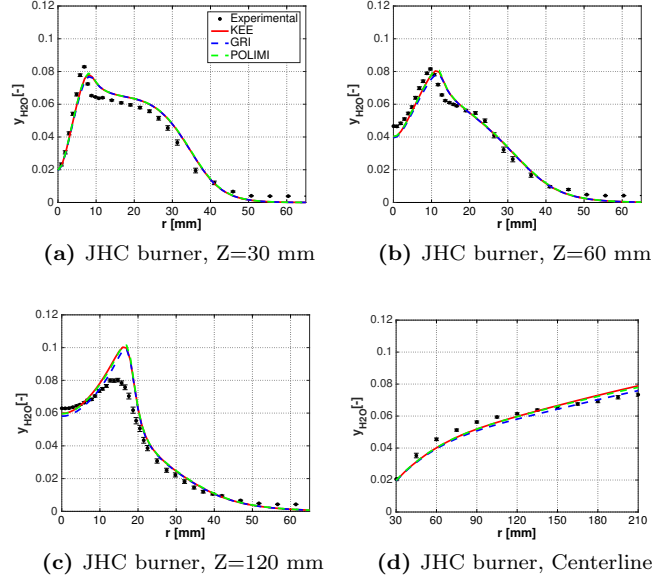
(a) JHC burner, Z=30 mm   **(b)** JHC burner, Z=60 mm

(c) JHC burner, Z=120 mm   **(d)** JHC burner, Centerline

Figure 7: Comparison of measured and computed H_2O mass fraction profiles at different locations, for JHC burner flameless combustion (modified k-epsilon)

Comparison of the three versions of the EDC

In this section, all the different versions of the Eddy Dissipation Concept are compared to each other using data from two different flames: the DLR/TU/Sandia $CH_4/H_2/N_2$ flame and the JHC burner flame. Figure 8 shows the radial temperature profiles for the DLR/A flame at different axial locations (a-e) and the axial profile (f) obtained using the three different formulations of the EDC and plotted against the experimental data. The temperature profiles collapsed well with the experimental data for all three runs. However, from the profile of NO mass fractions in Figure 9, the "EDC_old" formulation is able to alleviate the over-predictions of the NO mass fraction at all locations.

The different versions of EDC model have also an effect on the simulation results for the JHC burner. From Fig. 10, the "EDC_new" version shows closer results compared with the experimental values. While obvious deviation can be captured with the other versions of the EDC model. This indicates a strong interaction between the combustion and turbulence model formulations. In the "EDC_new" version of EDC, the reduced mass exchange between the fine structures and the surroundings compensates the over-estimated round jet spreading.

Conclusion

The numerical modelling of turbulent combustion is a very challenging task as it combines the complex phenomena of turbulence and chemical reactions. This study becomes even more challenging when large detailed kinetic mechanisms are used in order to understand some special features such as pollutant formation. In the present work, a new stable OpenFOAM solver for turbulent combustion capable of using detailed chemical reaction mechanisms was validated. Both the steady-state and the unsteady form of the solver were used for validation. The solver was tested against high-fidelity data of several Sandia flames (flames A, B and D) and the JHC burner flame. The simulations were performed using different level of detail in the kinetics by selecting different small and large mechanisms.

Results from the validation show generally satisfactory agreement between the numerical predictions and the experimental data, especially for the temperature and major species fraction profiles, even though some discrepancies on minor species like NO can be observed. The comparative study has been made between the three different formulations of the EDC model proposed over the years. The "EDC_old" version of the EDC model showed to be the most accurate for Sandia flames, even if the discrepancies between all three models are not very large. For the JHC burner flame, EDC version of "EDC_new" performs the best, while the other two formulations show obvious deviation.
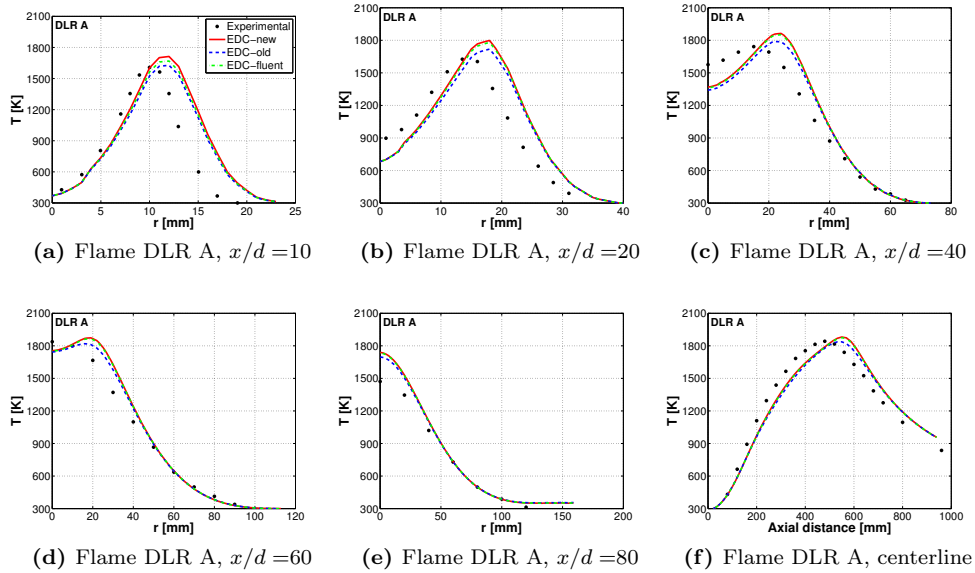

(a) Flame DLR A, x/d =10   (b) Flame DLR A, x/d =20   (c) Flame DLR A, x/d =40

(d) Flame DLR A, x/d =60   (e) Flame DLR A, x/d =80   (f) Flame DLR A, centerline

Figure 8: Comparison of measured and computed temperature profiles at different locations, for flame DLR A
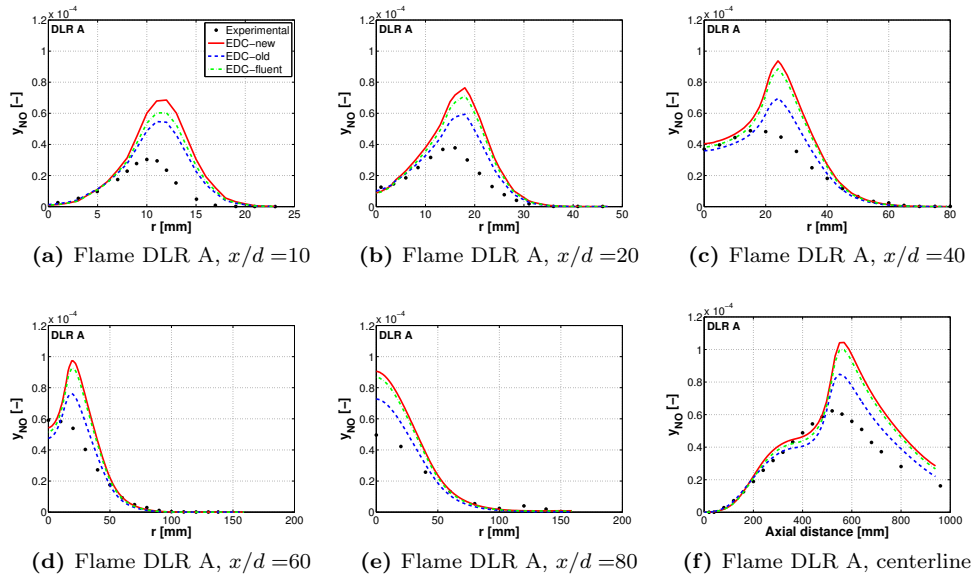
Figure 9: Comparison of measured and computed NO mass fraction profiles at different locations, for flame DLR A
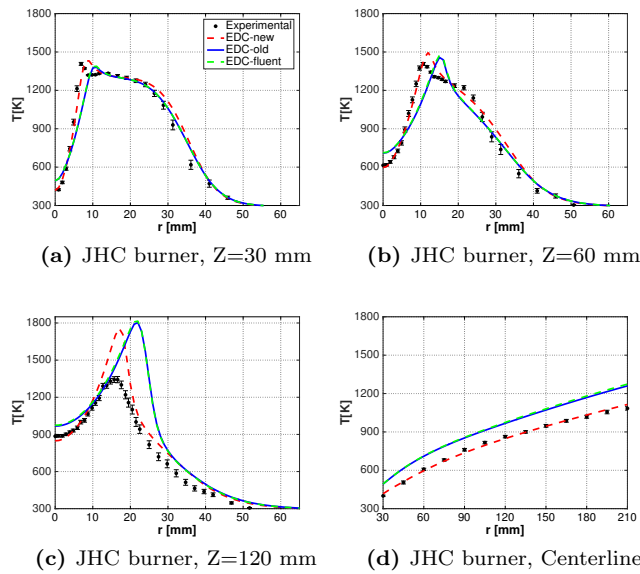

Figure 10: Comparison of measured and computed temperature profiles at different locations, for JHC burner flameless combustion

References

[1] Magnussen, B.F., "The eddy dissipation concept, a bridge between science and technology", *Eccomas Thematic Conference on Computational Computation* (2005).

[2] Cuoci, A., Frassoldati, A., Faravelli, T., Ranzi, E., "Opensmoke: Numerical modeling of reacting systems with detailed kinetic mechanisms", *XXXIV Meeting of the Italian Section of the Combustion Institute* (2011).

[3] Magnussen, B.F., "On the structure of turbulence and a generalized eddy dissipation concept for chemical reaction in turbulent flow", *19th AIAA Aerospace Science Meeting* (1981).

[4] Magnussen, B.F., "Modeling of nox and soot formation by the eddy dissipation concept", *Int. Flame Research Foundation, 1st topic Oriented Technical Meeting* (1989).

[5] Magnussen, B.F., Hjertager, B.H., "On mathematical models of turbulent combustion with special emphasis on soot formation and combustion", *Proc. Comb. Inst.* (1976).

[6] Ertesvg, I.S., Magnussen, B.F., "The eddy dissipation turbulent energy cascade model", *Combustion Science and Technology* pp. 213–236 (2001).

[7] Gran, I.R., Magnussen, B.F., "A numerical study of a bluff-body stabilized diffusion flame. part 2. influence of combustion modeling and finite-rate chemistry", *Combustion Science and Technology* pp. 191–217 (1996).

[8] Smith, G.P., Golden, D.M., Frenklach, M., Moriarty, N.W., Eiteneer, B., Goldenberg, M., Bowman, C.T., Hanson, R.K., Song, S., Jr., W.C.G., Lissianski, V.V., Qin, Z.

[9] Frassoldati, A., Faravelli, T., Ranzi, E., "Kinetic modeling of the interactions between no and hydrocarbons at high temperature", *Combust. Flame* 135:97–112 (2003).

[10] Barlow, R.S., Fiechtner, G.J., Carter, C.D., Chen, J., "Experiments on the scalar structure of turbulent CO/H2/N2 jet flames", *Combust. Flame* 120:549–569 (2000).

[11] Flury, M., *Experimentelle Analyse der Mischungstruktur in turbulenten nicht vorgemischten Flammen*, Ph.D. thesis, ETH Zurich, Switzerland (1998).

[12] Barlow, R.S., "Sandia/ETH-Zurich CO/H2/N2 flame data - release 1.1", (2002), URL www.ca.sandia.gov/TNF.

[13] Cuoci, A., Frassoldati, A., Faravelli, T., Ranzi, E., "Formation of soot and nitrogen oxides in unsteady counterflow diffusion flames", *Combust. Flame* 156:2010–2022 (2009).

[14] Bergmann, V., Meier, W., Wolff, D., Stricker, W., "Application of spontaneous raman and rayleigh scattering and 2d lif for the characterization of a turbulent ch4=h2=n2 jet diffusion flame", *Appl. Phys. B: Lasers Opt.* 66:489–502 (1998).

[15] Barlow, R.S., "Sandia H2/He flame data - release 2.0", (2003), URL http://www.ca.sandia.gov/TNF.

[16] Barlow, R.S., Carter, C.D., *Combust. Flame* 97:261–280 (1994).

[17] Barlow, R.S., Carter, C.D., *Combust. Flame* 104:288–299 (1996).

[18] Dally, B.B., Karpetis, A.N., Barlow, R.S., "Structure of turbulent non-premixed jet flames in a diluted hot coflow", *Proc. Comb. Inst.* 29:1147–1154 (2002).

[19] Bilger, R., Starner, S., Kee, R., "On reduced mechanisms for methane-air combustion in non-premixed flames", *Proc. Comb. Inst.* 29:1147–1154 (2002).

[20] "Chemical-kinetic mechanisms for combustion applications", URL http://combustion.ucsd.edu.

[21] Parente, A., Malik, M.R., Contino, F., Cuoci, A., Dally, B.B., "Extension of the eddy dissipation concept for turbulence/chemistry interactions to mild combustion", *Fuel* 163:98–111 (2015).